

# From Fe<sub>3</sub>Si towards Fe<sub>3</sub>Ge in Finemet-like nanocrystalline alloys: Mössbauer spectroscopy

J.A. Moya\*, V.J. Cremaschi, H. Sirkin

*Laboratorio de Sólidos Amorfos, Departamento de Física, Facultad de Ingeniería, Universidad de Buenos Aires and CONICET, Paseo Colón 850, (1063) Buenos Aires, Argentina*

## Abstract

Nanocrystalline Finemet-type ribbons with different Si/Ge ratio [Fe<sub>73.5</sub>Si<sub>13.5-x</sub>Ge<sub>x</sub>Nb<sub>3</sub>B<sub>9</sub>Cu<sub>1</sub> ( $x = 7, 8, 10$  and  $13.5$ )] were studied by means of Mössbauer spectroscopy and X-ray diffraction. The trend to form the non-stoichiometric DO3 Fe<sub>3</sub>Si structure in Finemet alloys ( $x = 0$ ) is confirmed as Si is substituted for Ge. Results also indicate that the crystalline fraction increases when Si is gradually replaced with Ge. The hyperfine magnetic fields and the isomer shifts are characterised by a quasi-linear relationship with the Ge content of the nanocrystals.

© 2006 Elsevier B.V. All rights reserved.

*Keywords:* Finemet; Nanocrystalline alloys; Mössbauer spectroscopy

## 1. Introduction

Finemet is the commercial name for a very well known nanocrystalline FeSiB-based alloy. It is obtained by partial devitrification of amorphous ribbons which leads to a structure that consists of ultra-fine crystalline grains embedded in an amorphous matrix. Since its discovery several authors have studied the influence of the addition of different elements with the aim of improving the magnetic, mechanical and chemical responses [1]. Suzuki and Blázquez have recently reported that the addition of Ge to the Fe<sub>89</sub>Zr<sub>7</sub>B<sub>3</sub>Cu<sub>1</sub> alloy improved the soft magnetic behaviour at high temperature by enhancing the Curie temperature  $T_C$  [2].

During the past years we have studied the influence of the partial substitution of Ge for Si in the Finemet alloy. Interesting results were found: a decrease in the coercivity, an increase in the permeability and saturation magnetization, a decrease of the first crystallization temperature and an increase in the boride crystallization temperature within a limited composition range and finally an increase in the  $T_C$  [3,4].

The Fe–Si and Fe–Ge systems present the Fe<sub>3</sub>Si and Fe<sub>3</sub>Ge DO3 structure, respectively. In Fig. 1, Fe atoms in A sites are represented by black circles, the 4 Si (Ge) atoms and 4 Fe atoms in D sites are represented by grey circles and open circles, respectively. In the case of non-stoichiometric DO3 structures with lower Si (Ge) content, some of the D sites are randomly occupied with Fe, resulting in different Fe environments. Fe atoms in D sites have 8 Fe atoms as nearest neighbours ( $n$ ), and 0–6 Si (Ge) atoms as next-nearest neighbours ( $m$ ) (sites D0–D6 respectively).

Fe atoms in A sites could have 0–4 Si (Ge) (A0–A4 sites) atoms as nearest neighbours ( $n = 0–4$ ) and have 6 Fe atoms as next-nearest neighbours ( $m = 6$ ). It has been possible to distinguish up to six different Zeeman sextets related to different Fe environments in Finemet-like alloys when fitting their Mössbauer spectra [5]. The probability of occurrence of each kind of Fe environment can be calculated using a binomial distribution [5] and depends on the Si (Ge) content. This fact is taken into account when calculating the chemical composition of the nanograins.

In this paper we present the preliminary Mössbauer spectroscopy (MS) and XRD studies on Finemet-like Fe<sub>73.5</sub>Si<sub>13.5-x</sub>Ge<sub>x</sub>Nb<sub>3</sub>B<sub>9</sub>Cu<sub>1</sub> ( $x = 6, 8, 10$  and  $13.5$ ) alloys

\*Corresponding author. Fax: +5411443311852.

E-mail address: [jmoya@fi.uba.ar](mailto:jmoya@fi.uba.ar) (J.A. Moya).

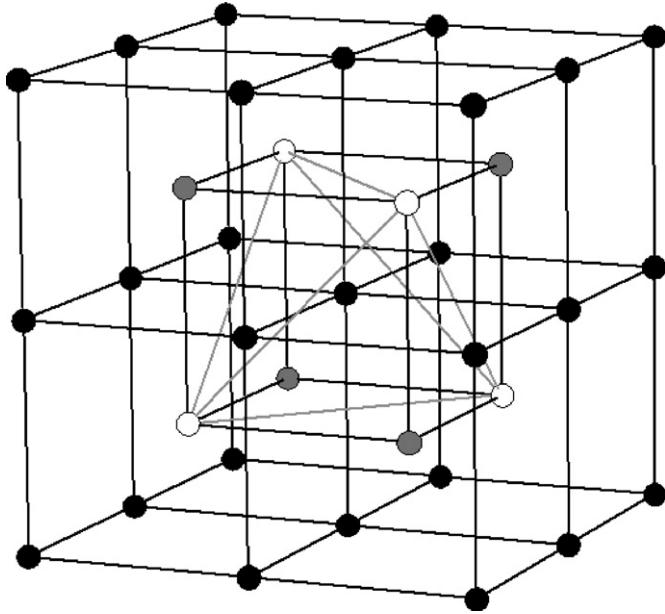


Fig. 1. Stoichiometric  $\text{Fe}_3\text{Si}$  (or  $\text{Fe}_3\text{Ge}$ ) DO3 lattice: A Sites denoted by full circles, D sites occupied by Fe in grey circles and D sites occupied by Si (or Ge) in open circles.

paying special attention to the passage from  $\text{Fe}_3\text{Si}$  to  $\text{Fe}_3\text{Ge}$  in non-stoichiometric DO3 structure.

## 2. Experimental

Nanocrystalline  $\text{Fe}_{73.5}\text{Si}_{13.5-x}\text{Ge}_x\text{Nb}_3\text{B}_9\text{Cu}_1$  ( $x = 7, 8, 10$  and  $13.5$ ) ribbons were obtained from the partial devitrification of their amorphous precursor alloys (prepared using the melt-spinning technique) after isothermal annealing for 1 h at  $540^\circ\text{C}$  (i.e. when all the alloys were nanocrystallized).

X-ray diffraction (XRD) was performed with a Rigaku diffractometer with monochromatized  $\text{Cu K}\alpha$  radiation. Information about lattice parameters were obtained from these patterns. MS was carried out in transmission geometry using a  $^{57}\text{Co}$  in Rh source. The calibration was performed with an  $\alpha\text{-Fe}$  foil. The isomer shifts (IS) are given relative to  $\alpha\text{-Fe}$ . The spectra fittings were performed using the NORMOS programs, DIST and SITE versions [6]. The DIST version allows to combine distributed hyperfine magnetic parameters (useful for amorphous phases) with up to five crystalline subspectra, while the SITE version only allows fitting discrete subspectra. The amorphous phase in partially nanocrystallised samples was evaluated employing both versions: SITE, using two wide sextets, and DIST, using two Gaussian distributions with a linear dependence of the hyperfine magnetic field  $B_{\text{hf}}$  on the isomer shift IS. Comparison between both kinds of fittings did not show markedly significant changes in the hyperfine parameters of samples annealed at  $540^\circ\text{C}$ . Hence we herein report the results obtained using the SITE program that allows employing six sextets to analyse the nanocrystalline phases.

## 3. Results

As an example we present in Fig. 2, the Mössbauer spectrum and its fitting for the sample  $\text{Ge}_{13.5}$  annealed at  $540^\circ\text{C}$ . The six subspectra of the crystalline phase, associated with different Fe coordinations ( $n, m$ ), are shown in different line styles and the residual amorphous phase is marked by the two shadowed subspectra. Fig. 3 depicts the whole behaviour of  $B_{\text{hf}}$  in samples varying their Ge content. As can be seen, all the  $B_{\text{hf}}$  roughly coincide when they are displayed as a function of  $n$  and  $m$ . The  $B_{\text{hf}}$  decreases as the number of Si or Ge nearest neighbour atoms ( $n$ ) increases. The dotted line in Fig. 3 was extrapolated to  $B_{\text{hf}}(5, 0) = 0$  where no magnetic interaction is expected [7]. The  $B_{\text{hf}}$  of the residual amorphous intergranular phase presented low values due to the high proportion of non-magnetic atoms [8]. According to the literature the highest value of  $B_{\text{hf}}$  of the residual

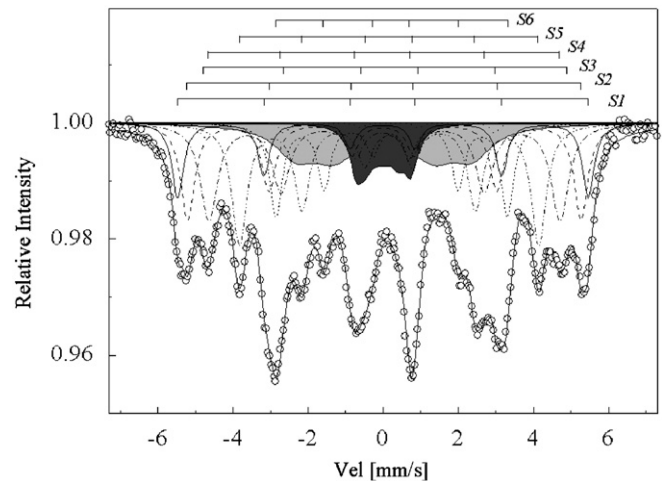


Fig. 2. MS and fitting of sample  $\text{Ge}_{13.5}$  annealed at  $540^\circ\text{C}$ .

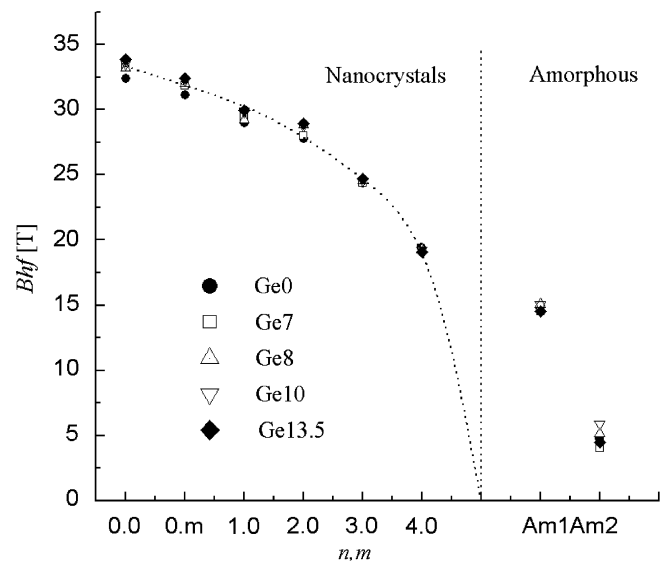


Fig. 3.  $B_{\text{hf}}$  of crystalline sites as a function of Fe  $n$  and  $m$  neighbours.  $B_{\text{hf}}$  of amorphous matrix is also reported (Am1 and Am2).

amorphous corresponds to Fe atoms located at the centre of the inter-nanograin amorphous region (rich in Fe) and the lowest value corresponds to Fe atoms of the amorphous remainder which are in close contact with the nanograins that suffered a Fe depletion during the nanocrystallisation [8].

On the other hand we found a continuous (quasi-linear) increase of  $B_{hf}$  and IS with the nominal Ge content of the alloys. For a better analysis we attempted to obtain the Si and Ge content of the nanograin crystalline phase from the relative resonant absorption area of sextets S1–S4, S5 and S6. The results of this analysis were 18.5% Si for sample Ge0 and 18.2% Ge for Ge13.5, and 18.8%, 19.0% and 18.55% (Si+Ge) for samples Ge7, Ge8 and Ge10, respectively, (the estimated error was  $\pm 1\%$ ). The problem at this point was to determine the %Si and %Ge separately of samples Ge7, Ge8 and Ge10. From XRD we could obtain the lattice parameter,  $a$ , of the different samples: for sample Ge0  $a = 5.676 \text{ \AA}$  and for sample Ge13.5  $a = 5.768 \text{ \AA}$ . A linear relationship between %Ge in the nanograins and  $a$  is expected when Si is substituted for Ge in the  $\text{Fe}_3\text{Si}$  structure finally leading to  $\text{Fe}_3\text{Ge}$ . With this assumption it was possible to obtain the %Ge in alloys with Si and Ge content. These results are tabulated in Table 1.

Then we plotted  $B_{hf}$  and IS as a function of the %Ge content in the nanograins. This is shown in Fig. 4. where an almost-linear dependence with %Ge was found for both parameters (for the  $B_{hf}$  only sites S1–S3 are shown). We also plotted the  $B_{hf}(0,0)$  data obtained by Dubiel and Zinn [9] with the  $\text{Fe}_{100-x}\text{Ge}_x$  alloy where a similar trend was observed in spite of the difference between both alloys: i.e. the use of Ge to replace Si in our case and the use of Ge to replace Fe in the case of Ref. [9]. In agreement with Ref. [9] we can state that substituting Ge for Si results in an increment in the spin-down s-electron density (and the s-electron charge density according to the IS results). It was also found that substituting Ge for Si in the Finemet alloy decreased the crystallization temperature [4] and reduced the amount of amorphous matrix. In Fig. 5 we report the %area corresponding to the Fe in amorphous phase ( $A_{m1} + A_{m2}$ ) as a function of the nominal %Ge content. The monotonous decrease in %area as Si was replaced with Ge (assuming the same recoilless factor for nanocrystalline and amorphous matrix) indicates a reduction of the amorphous matrix amount that involves an additional reduction in the Fe content of that matrix. Nevertheless,

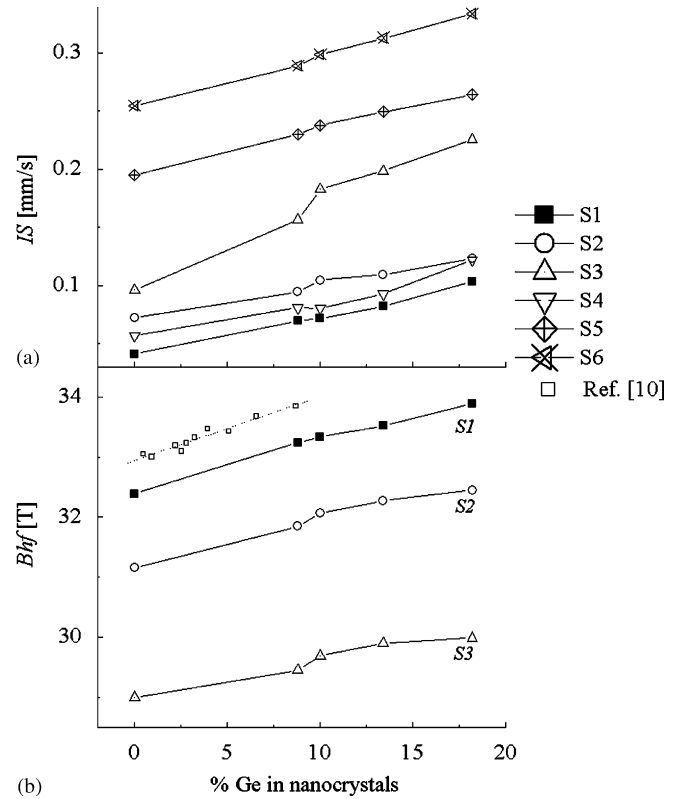


Fig. 4. IS (a) and  $B_{hf}$  (b) of crystalline sites as a function of the calculated at% Ge in nanograins. In graph (b) is also reported the data obtained by Dubiel and Zinn [9] as open square in order to compare.

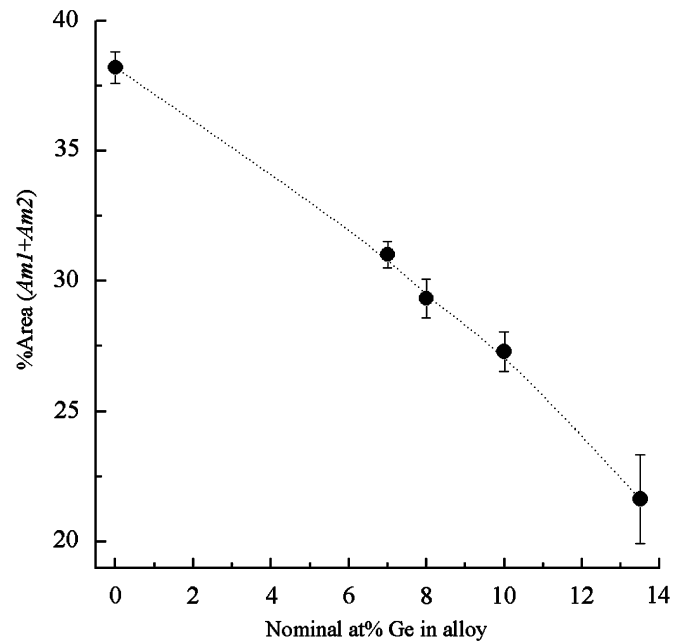


Fig. 5. Behaviour of %area of amorphous phase ( $A_{m1} + A_{m2}$ ) as Si is substituted for Ge (in nominal %Ge).

Table 1  
Lattice parameter,  $a$ , of nanocrystals obtained by XRD, atomic fraction of Ge and Si obtained from MS, % (Si + Ge) and at% of Ge, %Ge

Sample	Nominal (%Ge)	$a$ (Å) (XRD data)	% (Si + Ge) (MS data)	%Ge (XRD + MS)
Ge0	0	5.676	18.5	0
Ge7	7	5.721	18.8	8.8
Ge8	8	5.7272	19.0	10
Ge10	10	5.744	18.55	13.4
Ge13.5	13.5	5.768	18.2	18.2

the  $B_{hf}$  of the amorphous phase did not seem to vary significantly in any of the compositions when annealing at  $540^\circ\text{C}$  and their IS presented only a slight increase. Deeper studies on the amorphous matrix will be presented in future.

#### 4. Conclusion

The transition from  $\text{Fe}_3\text{Si}$  to  $\text{Fe}_3\text{Ge}$  non-stoichiometric structure in  $\text{Fe}_{73.5}\text{Si}_{13.5-x}\text{Ge}_x\text{Nb}_3\text{B}_9\text{Cu}_1$  ( $x = 7, 8, 10$  and  $13.5$ ) amorphous ribbons annealed at  $540^\circ\text{C}$  was studied and the %Ge and %Si content of the resulting nanocrystalline phase was calculated by means of XRD and MS. The same behaviour of  $B_{\text{hf}}(n,m)$ , the hyperfine magnetic field at the different Fe sites, was observed in all samples. The nanocrystalline phase increases at the expense of the amorphous phase and the  $B_{\text{hf}}(n,m)$  and the  $\text{IS}(n,m)$  of the former showed a quasi-linear increase when Si was replaced with Ge. The decrease in the quantity of amorphous matrix and the ensuing Fe depletion may be the cause of the decline of the soft magnetic properties of samples Ge10 and Ge13.5 [4].

#### References

- [1] M. Vázquez, J. Moya, V. Cremaschi, B. Arcondo, H. Sirkin, in: S.G. Pandalai (Ed.), Recent research Development in Nanostructures, vol. 1, Research Signpost, London, 1999, pp. 43–62.
- [2] K. Suzuki, et al., J. Appl. Phys. 91 (2002) 8417; J.S. Blázquez, S. Rotha, A. Conde, J. Magn. Magn. Mater. 290–291 (2005) 1589.
- [3] V. Cremaschi, et al., Physica B 320 (2002) 281; A. Saad, V. Cremaschi, H. Sirkin, J. Metast. Nanocryst. Mater. 20–21 (2004) 717.
- [4] V. Cremaschi, G. Sánchez, H. Sirkin, Physica B 354 (2004) 213.
- [5] G. Rixecker, P. Schaaf, U. Gonser, Phys. Status Solidi A 139 (1993) 309.
- [6] R.A. Brand, Normos Program, Internal Report, Angewandte Physik, Universität Duisburg, 1987.
- [7] A.F. Cabrera, F.H. Sánchez, Phys. Rev. B 65 (2002) 094202.
- [8] J.M. Borrego, C.F. Conde, A. Conde, J.M. Greneche, J. Phys.: Condens. Matter 14 (2002) 883.
- [9] S.M. Dubiel, W. Zinn, Phys. Rev B 28 (1983) 67.